

000 001 002 003 004 005 006 007 008 009 010 011 012 013 014 015 016 017 018 019 020 021 022 023 024 025 026 027 028 029 030 031 032 033 034 035 036 037 038 039 040 041 042 043 044 045 046 047 048 049 050 051 052 053 MOLD: FINE-GRAINED MULTIMODAL RISK ASSESS- MENT VIA DYNAMIC ANALYSIS WEIGHTS

Anonymous authors

Paper under double-blind review

ABSTRACT

Current multimodal AI safety detection often lacks granularity, interpretability, and adaptability. To address these limitations, we introduce **MoLD** (Mixture of LoRA Detectors), a framework that uniquely assesses risk by dynamically analyzing the interplay of multiple Low-Rank Adaptation (LoRA) module weights. This approach yields fine-grained, interpretable assessments beyond binary classification, enables concurrent **multi-risk detection**, maintains robustness on long-sequence data, and supports low-cost modularity. Impressively, MoLD demonstrates state-of-the-art (**SOTA**) performance on textual and visual benchmarks while achieving exceptional **few-shot** learning, reducing data requirements by over **90%**. Thus, MoLD provides a powerful, scalable, and data-efficient path to robust, interpretable risk assessment in large-scale multimodal AI systems.

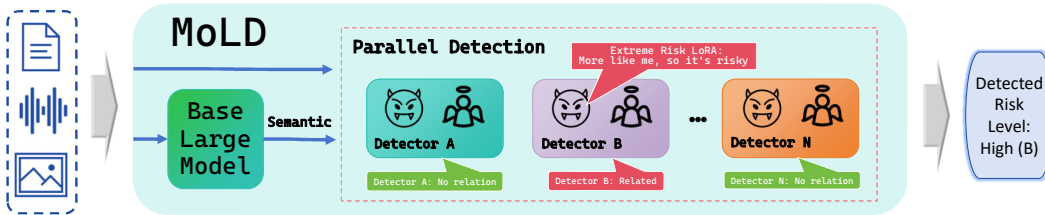


Figure 1: The Teaser Figure of MoLD

1 INTRODUCTION

While the internet has revolutionized communication and knowledge sharing Singh et al. (2022a), it has also facilitated a surge in harmful online content—spanning text, images, and other media—such as hate speech and harassment Garg et al. (2023), negatively impacting users and digital environments Kowalski (2018). Unchecked, these multifaceted issues can escalate into severe social conflicts Ezeibe (2021). Consequently, automated content moderation has become a vital research focus. Early efforts, and much subsequent research, concentrated on text security analysis using Natural Language Processing (NLP) Blodgett et al. (2020); Garrido-Muñoz et al. (2021); Weidinger et al. (2021) given the prevalence and complexity of textual data.

Manual content moderation on social platforms struggles with scale, cost, and subjectivity Young (2022); Aroyo et al. (2019). To automate detection, early machine learning approaches evolved from traditional classifiers like SVMs Singh et al. (2023) and CNNs Singh et al. (2022b) to supervised models Burdisso et al. (2019), but these single-task methods lacked multitasking flexibility. Although multi-label classifiers Gunasekara & Nejadgholi (2018); Cai et al. (2024) could address multiple toxicity types, their practical use was limited by the need for complete retraining and large labeled datasets for new categories Zinov'yeva et al. (2020).

However, persistent limitations, particularly in handling long-form content Zinov'yeva et al. (2020); Caselli et al. (2020) and cohesively assessing diverse online risk modalities, highlight a critical need for a new risk assessment paradigm. Such a paradigm should offer nuanced, interpretable, and data-efficient insights while scaling effectively across various modalities and evolving risks.

To address these limitations, we introduce MoLD, a novel weight-centric framework. MoLD dynamically analyzes multiple groups of LoRA modules, each of which represents a distinct risk theme and contains several LoRAs fine-tuned for different extreme tendencies, in order to uncover subtle risk signals. This enables nuanced, interpretable profiling beyond binary classification, alongside robust few-shot performance. MoLD thus offers a practical, data-efficient tool for large-scale multimodal risk assessment and points towards more adaptable and understandable AI safety mechanisms.

The main contributions of our method are:

- 1. Fine-Grained Multimodal Risk Assessment:** The framework introduces a novel, weight-centric approach that analyzes dynamic LoRA weights to provide nuanced and interpretable risk profiles for various content modalities like text and images, moving beyond simple binary classifications.
- 2. High Data and Parameter Efficiency:** MoLD demonstrates exceptional few-shot learning capabilities, reducing training data requirements by over 90%. Its modular design allows for the addition of new risk dimensions with negligible parameter overhead, ensuring scalability.
- 3. Efficient & Concurrent Multi-Risk Monitoring:** The system is designed to assess multiple, complex risk themes in parallel within a single analytical pass. Its high computational efficiency is maintained across both short-form and long-sequence content, making it ideal for scalable, real-world deployment scenarios.

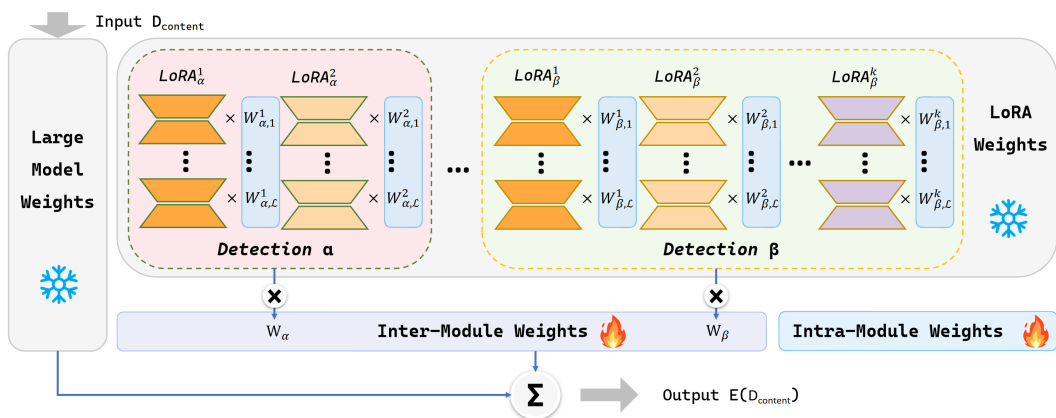


Figure 2: Architecture of MoLD.

2 METHODOLOGY

2.1 OVERVIEW

This chapter details the MoLD framework, illustrated in Figure 2. At its core, MoLD leverages a base large model for semantic understanding and assesses multimodal content by dynamically optimizing scalar weights for its detection modules. Each detection module is composed of a set of pre-trained LoRA adapters, where each adapter embodies a different extreme tendency of a defined risk theme. The final optimized weights serve as a quantitative measure, indicating both the relevance of each risk theme and the input's specific tendency within those themes.

2.2 MOLD ARCHITECTURE

MoLD utilizes a frozen pre-trained base model (M) augmented by N detection modules. Each module i (where $i = 1, 2, \dots, N$) employs a set of frozen LoRAs ($L_i^1, L_i^2, \dots, L_i^k$), each pre-trained on a different extreme tendency of its theme, thereby focusing the base model's semantic analysis on that specific risk theme.

To assess a given data content, D_{content} (e.g., an image or text under analysis), MoLD determines the appropriate contribution from each LoRA module by optimizing multiple dynamic scalar weights during the analysis phase:

- **Inter-Module Weights(w_i):** For each dimension i , w_i signifies its overall relevance of that dimension to the assessed D_{content} . These weights are constrained to sum to 1 across all N dimensions (Equation 1), indicating which dimensions are most pertinent to the input.

$$\sum_{i=1}^N w_i = 1 \quad (1)$$

- **Layer-Specific Intra-Module Weights($w_{i,l}^k$):** For each layer l in module i , the weights $w_{i,l}^k$ quantify the assessed D_{content} 's alignment with each of the module's defined tendencies (indexed by k). Constrained to sum to 1 per layer (Equation 2), they measure this layer-specific tendency.

$$\sum_{k=1}^{K_i} w_{i,l}^k = 1, \quad \forall l \in \{1, 2, \dots, \mathcal{L}\}, \quad \forall i \in \{1, 2, \dots, N\} \quad (2)$$

Where K_i is the number of LoRA adapters within module i , and $K \geq 2$, with each adapter representing a distinct tendency, and \mathcal{L} is the total number of LoRA layers.

2.2.1 INTEGRATING MULTIPLE DETECTION MODULES

Integrating N detection modules (thus $\sum_{i=1}^N K_i$ LoRA modules) with the base model M needs careful synthesis. Naive LoRA combination (e.g., linear weight summation) typically impairs performance and dilutes module specificity. MoLD mitigates this via a hierarchical weighted strategy (Equation 3): Dynamic Intra-Module weights modulate the layer-specific contributions of LoRAs within each thematic group, while Inter-Module weights scale the overall influence of each theme-specific module.

$$E(D_{\text{content}}) = M(D_{\text{content}}) + \sum_{i=1}^N \underbrace{w_i}_{\text{Inter-Module}} \cdot \sum_{k=1}^{K_i} \sum_{l=1}^{\mathcal{L}} \underbrace{w_{i,l}^k \cdot L_{i,l}^k(D_{\text{content}})}_{\text{Intra-Module}} \quad (3)$$

2.3 LoRA MODULE PRE-TRAINING

The foundation of MoLD's assessment capability lies in its specialized LoRA modules. For each defined risk theme i , a corresponding set of K_i LoRA is pre-trained. Each adapter is fine-tuned on a curated dataset representing a specific extreme tendency of that theme.

The rationale for using extreme tendencies is twofold.

1. Using extreme tendencies maximizes the discriminative power of each LoRA adapter and establishes a more expressive semantic basis.
2. By representing novel content as a compositional interpolation of these well-defined extremes, the resulting assessment becomes more fine-grained and interpretable.

This pre-training process is a one-time, offline procedure. Once completed, the weights of the base model (M) and all LoRA are frozen. They are not updated during the subsequent risk assessment phase. This clear separation between training and inference ensures that the assessment process is lightweight and fast.

2.4 INFERENCE PROCESS

When a new piece of content, D_{content} (e.g., text or an image), is presented for analysis, MoLD performs a rapid, online optimization process to determine the optimal dynamic scalar weights (w_i and $w_{i,l}^k$).

162 This process is framed as an inverse problem: what set of weights best configures the frozen model
 163 to explain the given content?

164 The optimization is achieved by minimizing the model’s own task loss directly on the content
 165 D_{content} . For instance, for a Large Language Model, the objective is to minimize the negative
 166 log-likelihood of the content. For an image model, this could be the mean squared error of
 167 reconstruction. The loss function is minimized exclusively with respect to the dynamic weights:

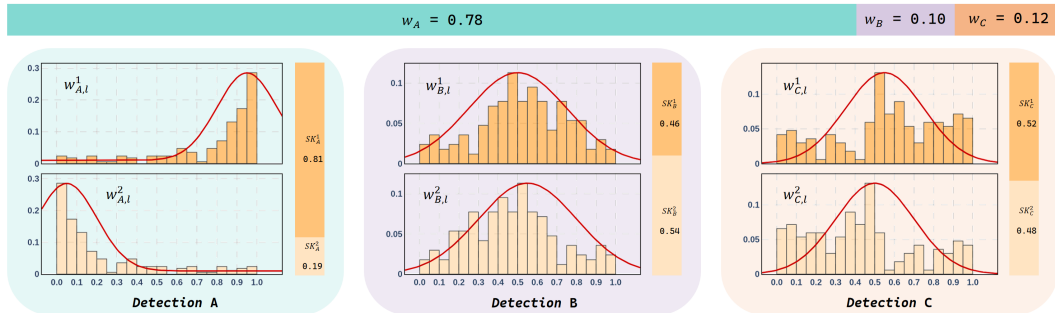
$$\min_{w_i, w_{i,l}^k} \text{Loss}(E(D_{\text{content}}), D_{\text{content}}) \quad (4)$$

172 The resulting optimized weights (w_i and $w_{i,l}^k$) form the basis of the final risk classification, as they
 173 directly encode the input’s alignment with the pre-defined risk themes and tendencies.

174 2.5 ANALYZING WEIGHTS FOR RISK DETECTION

175 Having established MoLD’s architecture and the dynamic weight optimization process, we now
 176 detail how these weights are systematically analyzed to perform risk detection. The analysis involves
 177 two layers:

- 180 1. Determining the relevance of each risk theme via Inter-Module weights.
- 181 2. Identifying the specific dominant tendency within the relevant themes via Intra-Module
 182 weights.



195 Figure 3: The distribution of weights. Top: Inter-Module Weights, Bottom: Intra-Module Weights
 196 Histogram. The histogram is the frequency of the layers of the weight distribution in every 0.05 bin.
 197

198 2.5.1 INTRA-MODULE WEIGHT BIAS ANALYSIS

200 While Inter-Module weights indicate relevant dimensions, Intra-Module weights show the input’s
 201 tendency toward an extreme within a dimension i . To quantify this directional bias, MoLD analyzes
 202 the distribution of these layer-specific weights as follows:

- 204 1. **Intra-Module Weights Distribution:** For a given risk dimension i , consider one of its
 205 multiple LoRA modules. We analyze the distribution of its layer-specific Intra-Module
 206 weights. The $[0, 1]$ range of these Intra-Module weights is divided into discrete bins (e.g.,
 207 20 bins, each of width 0.05). The frequency (f_j) of weights falling into each bin j is
 208 then computed, forming a distribution (Figure 3, bottom) that reveals patterns of weight
 209 concentration.
- 210 2. **Calculate Modified Skewness** To quantify the directional bias of this distribution, a tai-
 211 lored measure of skewness, \hat{SK} , is computed. This metric measures asymmetry relative to
 212 the distribution’s center (0.5) by assigning a directional sign x_j to each bin’s frequency f_j .
 213 \hat{SK} is calculated as:

$$\hat{SK} = \frac{\frac{1}{n} \sum_{j=1}^n x_j \cdot f_j^3}{\sigma_f^3}, \quad x_j = \begin{cases} -1, & j \leq \lfloor \frac{n}{2} \rfloor \\ 1, & j > \lfloor \frac{n}{2} \rfloor \end{cases} \quad (5)$$

216

217 Here, n is the total number, f_j is the frequency of the j -th bin, and σ_f is the standard
 218 deviation of the frequency vector $f = \{f_1, \dots, f_n\}$. This metric effectively quantifies the
 219 directional activation bias for each LoRA module across layers.

220

221 **3. Normalize Tendencies Scores:** For each dimension i and each of its corresponding LoRA
 222 modules (indexed by k), a modified skewness score, \hat{SK}_i^k , is computed. Applying a soft-
 223 max function across all these scores for dimension i yields the final Intra-Module risk
 224 tendency scores, SK_i^k :

225

$$\{SK_i^k\}_{k=1}^{K_i} = \text{Softmax}(\{\hat{SK}_i^k\}_{k=1}^{K_i}) \quad (6)$$

227

228 These normalized scores sum to 1, representing the input's alignment strength towards the
 229 k extremes of dimension i .

230

231 2.5.2 FINAL RISK CLASSIFICATION

232

233 The final risk classification synthesizes dimension relevance (from Inter-Module weights w_i) and
 234 directional tendency (from Intra-Module scores SK_i^k). An input is flagged for a specific risk if both
 235 of the following conditions are met for a monitored dimension i :

236

1. **Sufficient Relevance:** The dimension i is identified as highly relevant to the input. This
 237 can be determined by its Inter-Module weight being maximal or exceeding a predefined
 238 relevance threshold θ_w .
2. **Significant Tendency:** The input demonstrates a strong alignment with one of the di-
 239 mension's extremes. This is confirmed if the corresponding Intra-Module tendency score
 240 (SK_i^k) surpasses a sensitivity threshold θ_{SK} .

242

243 If these conditions are not satisfied for any monitored dimension, the input is classified as benign
 244 concerning these specific risks. The thresholds (θ_w, θ_{SK}) are adjustable to tune the system's sensi-
 245 tivity and specificity for different application needs.

246

247 2.6 EFFICIENCY AND SCALABILITY ANALYSIS

248

249 A key advantage of the MoLD framework lies in its exceptional parameter efficiency and computa-
 250 tional scalability, particularly when monitoring multiple risk dimensions concurrently.

251

252 2.7 PARAMETER EFFICIENCY

253

254 Conventional approaches to multi-risk detection often require training and deploying a separate
 255 model for each risk type. For a system designed to detect N distinct risk themes, the total parameter
 256 count for such a baseline approach (P_{Baseline}) would scale linearly with N :

257

$$P_{\text{Baseline}}(N) \approx N \times P_{\text{model}} \quad (7)$$

258

259 where P_{model} is the number of parameters in a single, fully fine-tuned model.

260

261 In stark contrast, MoLD leverages a single, shared base model (M) and only adds a small set of
 262 lightweight LoRA adapters for each new risk theme. The total parameter count of the MoLD system
 263 (P_{MoLD}) is therefore:

264

$$P_{\text{MoLD}}(N) = P_{\text{base}} + \sum_{i=1}^N \sum_{k=1}^{K_i} P_{L_i^k} \quad (8)$$

265

266

267

268

269

270 where P_{base} is the parameter count of the large base model, and $\sum_{k=1}^{K_i} P_{L_i^k}$ is the total parameter
 271 count of the LoRA for theme i . Since LoRA adapters are extremely small by design (typically $<$
 272 0.1% of P_{base}), the growth in total parameters as N increases is negligible compared to the baseline.

270 271 272 273 274 275 276 277 278 279 280 281 282 283 284 285 286 287 288 289 290 291 292 293 294 295 296 297 298 299 300 301 302 303 304 305 306 307 308 309 310 311 312 313 314 315 316 317 318 319 320 321 322 323 2.8 COMPUTATIONAL EFFICIENCY AND PARALLELISM

MoLD’s efficiency extends to its inference-time computation. During the risk assessment for a given content D_{content} , the vast majority of the system’s parameters (both P_{base} and all P_{LoRA}) are frozen. The only parameters being optimized (P_{optim}) are the small sets of scalar weights:

$$P_{\text{optim}} = \underbrace{\sum_{i=1}^N (K_i \times \mathcal{L})}_{\text{Intra-Module}} + \underbrace{\sum_{i=1}^N (K_i \times \mathcal{L})}_{\text{Inter-Module}} \quad (9)$$

This number is exceptionally small (e.g., in the order of hundreds or a few thousands), allowing the optimization to converge rapidly.

Furthermore, the framework is inherently parallel. The optimization process solves for all P_{optim} simultaneously, meaning the input content is assessed against all N risk themes concurrently within a single analytical pass. This is a significant advantage over methods that would require N separate models to be loaded and run sequentially. This powerful parallel capability allows MoLD to produce a comprehensive, multi-faceted risk profile with minimal latency, making it an ideal solution for scalable, real-world content moderation systems.

3 EXPERIMENTS

3.1 DATASETS

To train the LoRA modules representing extremes and evaluate MoLD, datasets for selected textual and visual dimensions were curated and split into training, validation, and testing sets in a 6:2:2 ratio, respectively.

Textual Datasets:

We focused on three textual dimensions relevant to societal risks, bias, and style:

- **Gender Perspective:** ‘Feminism’, ‘Misogyny’.
- **Racial Attitude:** ‘Anti-Black’, ‘Pro-Black’.
- **Behavioral Style:** ‘Meticulous’, ‘Careless’, ‘Humor’.

Data for ‘Feminism’, ‘Misogyny’, ‘Humor’ and ‘Anti-Black’ categories were extracted from public datasets (ClimaConvoShiwakoti et al. (2024), ToxiGenHartvigsen et al. (2022), DHATEVidgen et al. (2020), and SBICV2Sap et al. (2019)).

Other categories (‘Pro-Black’, ‘Meticulous’, ‘Careless’) were synthetically generated via GPT-4oHurst et al. (2024) using specific prompts (see Table 1 for examples). All textual samples underwent filtering by a GPT-4o assessor (Table 1), retaining only those scoring $> 8/10$ for extremity, yielding 5,000 samples per extreme category.

Visual Datasets:

For the visual modality, we addressed dimensions related to content safety, and style:

- **Regulated Content:** ‘Violence’, ‘Sexual’, ‘Self-Harm’, ‘Discriminatory’.
- **Image Style:** ‘Cartoon’, ‘Realistic’.

Table 1: Templates for Large Language Model. Top: Used to generate synthesized data. Bottom: Used to rate the polarity of the content.

Prompt Instances

- **Prompt for data:** Generate a two-role (Questioner, Responder) dialogue corpus on open-ended/everyday topics. Questioner: Asks/opines curiously, doubtfully, or factually. Responder: Gives serious, goal-driven, detailed, clear, structured, practical, non-vague replies.

- **Prompt for score:** As a linguistic analyst, rate conversation meticulousness (Scale: 0=none to 10=extremely meticulous). Consider: Language, tone, context.

324 'Sexual', 'Violence', 'Discriminatory' and 'Self-Harm' data were curated from VHD11k Yeh et al.
 325 (2024) and UnsafeBench Qu et al. (2024). For 'Cartoon' and 'Realistic' categories, 100 images and
 326 50 short videos per category were collected from public online sources by the authors.
 327

328 3.2 EXPERIMENTAL SETUP

330 This section details the MoLD risk assessment configuration and the LoRA module training hyper-
 331 parameters. All experiments were conducted on a server equipped with 128GB of RAM and a single
 332 NVIDIA GeForce RTX 4090 GPU.
 333

334 3.2.1 MoLD RISK ASSESSMENT CONFIGURATION

335 For the risk assessment procedure detailed, we employed the following specific parameter settings
 336 across all experiments:
 337

- 338 • **Relevance Identification (Inter-Module Weights):** The most relevant risk dimension k
 339 was selected based on the maximum Inter-Module weight ($w_k = \max_i w_i$).
- 340 • **Tendency Evaluation (Intra-Module Weights):** A threshold $\theta_{SK} = 0.8$ determined sig-
 341 nificant directional bias. A value empirically set on a validation set.
 342

343 LoRA Module Training Details

344 Base Models:

- 346 • **NLP domain:** Qwen2.5-Instruct series Yang et al. (2024) (0.5B, 1.5B, 3B, 7B parameters)
- 347 • **V&L domain:** Pre-trained Stable Diffusion v2.1Rombach et al. (2021).

349 LoRA modules for each risk theme were trained independently with the following settings:

350 **NLP LoRAs (Qwen-based):** Learning rate 5e-5 (cosine scheduler), 5 epochs, batch size 8, rank 8,
 351 and α as 16.
 352

353 **Vision LoRAs (SD-based):** Image resolution 512x512, learning rate 1e-5, 400 iterations, batch size
 354 2, rank 4, and α as 0.5.
 355

356 3.3 MOLD ON NLP DOMAIN

357 This section evaluates MoLD's text-based risk detection
 358 via four experiments: few-shot learning, base-
 359 line comparison, variable text length handling,
 360 and multi-risk detection. Results use Qwen2.5-0.5B-
 361 Instruct as the base LLM unless stated otherwise.
 362 The dynamic weight optimization for each assess-
 363 ment was conducted over 5 iterations.
 364

365 3.3.1 FEW-SHOT 366 AND CROSS-SCALE PERFORMANCE

367 MoLD's ability to achieve strong performance with
 368 minimal training data was investigated.
 369

370 Cross-scale Consistency:

371 MoLD showed consistent high accuracy across
 372 Qwen2.5-Instruct sizes (0.5B-7B) when trained with
 373 few samples (e.g., 200 per extreme). The 0.5B
 374 model's few-shot performance matched larger models (Figure 4, top).
 375

376 Few-shot Learning vs. Baselines:

377 Compared to fine-tuning baselines (BERTDevlin et al. (2019), DistilBERTSanh et al. (2019),
 378 RoBERTaLiu et al. (2019), and ClimateBERTWebersinke et al. (2021)), MoLD (0.5B base) achieved

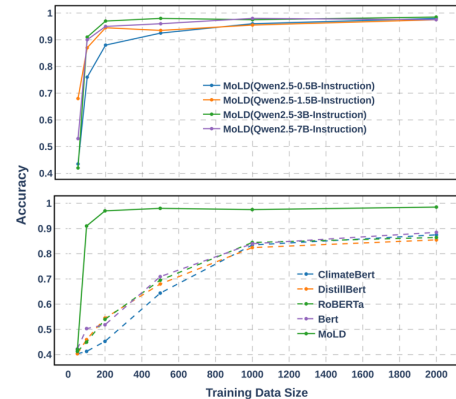


Figure 4: Comparison of MoLD with baselines at different data scales.

Top: MoLD's cross-scale consistency capability.
 Bottom: Few-shot learning capability of MoLD

378 near-peak accuracy (~ 0.96) with only 200 samples per extreme, while baselines needed ≥ 2000
 379 samples (Figure 4, bottom). MoLD required $> 90\%$ less training data. This highlights MoLD’s
 380 exceptional data efficiency, valuable for low-resource risk detection scenarios.
 381

382 3.3.2 COMPARISON OF BASELINE NLP MODELS

383 MoLD (trained on 200 samples per extreme)
 384 was benchmarked against strong NLP base-
 385 lines (BERTweet + Llama2Kaya et al. (2024),
 386 BERT, DistilBERT, RoBERTa, and Climate-
 387 BERT) trained on larger datasets.
 388

389 MoLD achieved a superior F1 score (0.959),
 390 surpassing all baselines (Table 2), demon-
 391 strating its competitive performance despite high
 392 data efficiency.

393 Table 3 presents the average inference time over
 394 100 test samples of 30 tokens each. The results
 395 show that while MoLD’s speed is comparable to
 396 the fastest baseline for 2-Risks detection, it holds
 397 a significant advantage in more complex multi-
 398 Risks (4 and 7) scenarios, demonstrating its ex-
 399 cellent scalability for parallel monitoring tasks.
 400

401 3.3.3 DETECTION ACROSS VARIABLE TEXT 402 LENGTHS

403 MoLD’s robustness to varying input lengths
 404 was tested by training on short texts (200 sam-
 405 ples, 200-400 chars) and evaluating on inputs
 406 from 200 to 4,000 characters.
 407

408 MoLD maintained high accuracy and recall
 409 across all lengths (Figure 5), demon-
 410 strating its ability to handle long-form content effec-
 411 tively without length-specific adaptations, un-
 412 like token-limited models.
 413

414 3.3.4 CONCURRENT MULTI-RISK 415 DETECTION

416 MoLD’s ability to monitor multiple risks sim-
 417 ultaneously was tested. Configured with LoRA
 418 modules for all three NLP dimensions (Seven ex-
 419 tremes) active concurrently.
 420

421 MoLD maintained high Precision, Recall, and
 422 Accuracy across all categories (Table 4), show-
 423 ing minimal interference between parallel detec-
 424 tion processes and confirming its scalability for
 425 multi-risk monitoring.
 426

427 3.4 MOLD ON V&L DOMAIN

428 This section evaluates MoLD’s visual risk detection capabilities, comparing it against baselines and
 429 testing concurrent multi-risk detection.
 430

431 3.4.1 COMPARISON OF BASELINE V&L MODELS

Table 2: NLP Model Performance Comparison.

Model	Acc	F1
BERT	0.901	0.708
DistilBERT	0.896	0.664
RoBERTa	0.842	0.662
ClimateBERT	0.884	0.704
BERTweet+Llama2	0.952	0.890
Optimal MoLD	0.96	0.959

Table 3: Inference Time Comparison.

Model	2-Risks	4-Risks	7-Risks
BERT	1882ms	3766ms	6580ms
DistilBERT	1027ms	2041ms	3570ms
RoBERTa	1467ms	2888ms	5048ms
ClimateBERT	1520ms	3005ms	5338ms
BERTweet+Llama2	1732ms	3123ms	6439ms
Optimal MoLD	1150ms	1546ms	1951ms

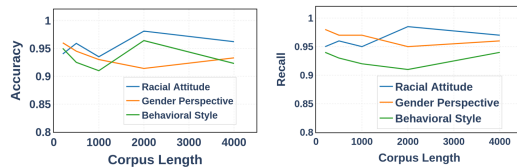


Figure 5: The performance of MoLD in detecting text of different lengths.

Table 4: MoLD performance for multiple text risk dimension simultaneously.

Risk Dimension	Precision	Recall	Accuracy
Feminism	0.989	0.98	0.99
Misogyny	0.925	0.99	0.985
Anti-Black	1.0	0.92	0.986
Pro-Black	0.943	1.0	0.99
Meticulous	0.923	0.96	0.98
Careless	1.0	0.92	0.986
Humor	0.956	0.934	0.976

432 MoLD’s performance on ’Violence’ vs. ’Self-
 433 Harm’ image detection was compared against
 434 baselines (LlavaGuardHelff et al. (2024), GPT-
 435 4o miniHurst et al. (2024), Gemma3Team et al.
 436 (2024) and SG2Zeng et al. (2025)).

437 MoLD was trained using only 40 images per ex-
 438 treme (tested on 60). MoLD achieved a superior
 439 F1 score of 0.901 (Table 5), surpassing reported
 440 baseline results on similar tasks. This high per-
 441 formance with minimal training data highlights MoLD’s strong data efficiency extending to the
 442 visual domain.

444 3.4.2 CONCURRENT MULTI-RISK DETECTION

446 MoLD’s capacity for simultaneous multi-risk vi-
 447 sual detection was evaluated. Configured with
 448 LoRA modules for two visual dimensions (six ex-
 449 tremes total) active concurrently.

450 MoLD maintained high performance (accuracy
 451 0.91 ~ 0.967) across all six categories simultane-
 452 ously (Table 6). This demonstrates effective con-
 453 current multi-risk visual assessment with mini-
 454 mal interference, confirming its robustness and
 455 potential for scalable visual safety monitoring.

456 3.4.3 DETECTION ON SEQUENTIAL VISUAL DATA (VIDEO)

458 To evaluate MoLD’s performance on sequential
 459 visual data, we tested its ability to detect risks
 460 in video clips. Each video was treated as a se-
 461 quence of image frames. The results (Table 7)
 462 show that MoLD maintains high accuracy, suc-
 463 cessfully identifying the video’s dominant. This
 464 demonstrates that the framework’s robustness to
 465 long-sequence data extends from the text to the visual domain.

466 3.5 ABLATION STUDY

468 We conduct ablation studies to validate two
 469 key components of MoLD: our modified skew-
 470 ness (SK) analysis and the hierarchical, layer-
 471 specific weight architecture. As shown in Table
 472 8, removing either component results in a sig-
 473 nificant performance drop.

474 Replacing the SK analysis with a simple aver-
 475 aging heuristic degrades the F1-score from
 476 0.959 to 0.895. The impact is more severe when
 477 removing the layer-weights, which lowers the F1-score to 0.823. These results confirm that both our
 478 SK-based analysis and the hierarchical weight structure are crucial for MoLD’s superior perfor-
 479 mance.

480 4 CONCLUSION

483 This work introduced MoLD, a novel framework for nuanced multimodal risk assessment that an-
 484 alyzes the dynamic interplay of specialized LoRA module weights. Experiments demonstrate that
 485 MoLD achieves state-of-the-art, scalable, and multi-dimensional risk detection with significant data
 and parameter efficiency.

Table 5: Comparison of MoLD with baseline
 V&L models

Model	Pre	Rec	F1
LlavaGuard	0.476	0.931	0.63
LlavaGuard(SG)	0.672	0.989	0.8
GPT-4o mini	0.683	0.977	0.803
Gemma3	0.777	0.879	0.825
SG2	0.876	0.897	0.886
Optimal MoLD	0.896	0.91	0.901

Table 6: MoLD detects results for multiple im-
 age risk dimensions simultaneously.

Risk Dimension	Precision	Recall	Accuracy
Violence	0.94	0.922	0.953
Sexual	0.91	0.903	0.91
Discriminatory	0.97	0.94	0.953
Self-Harm	0.985	0.92	0.967
Cartoon	0.99	0.93	0.96
Realistic	1.0	0.92	0.96

Table 7: MOLD performance on video risk de-
 tected.

Risk Dimension	Precision	Recall	Accuracy
Cartoon	1.0	0.96	0.98
Realistic	0.98	0.96	0.97

Table 8: Ablation studies on core components of
 MoLD.

Model Variant	Acc	Pre	Rec	F1
Full MoLD	0.960	0.962	0.956	0.959
w/o SK (Avg.)	0.915	0.906	0.887	0.895
w/o Layer-Weights	0.831	0.840	0.806	0.823

486 REFERENCES
487

488 Nouar AlDahoul, Myles Joshua Toledo Tan, Harishwar Reddy Kasireddy, and Yasir Zaki. Advanc-
489 ing content moderation: Evaluating large language models for detecting sensitive content across
490 text, images, and videos. *arXiv preprint arXiv:2411.17123*, 2024.

491 Lora Aroyo, Lucas Dixon, Nithum Thain, Olivia Redfield, and Rachel Rosen. Crowdsourcing
492 subjective tasks: The case study of understanding toxicity in online discussions. In *Compan-
493 ion Proceedings of The 2019 World Wide Web Conference*, WWW '19, pp. 1100–1105, New
494 York, NY, USA, 2019. Association for Computing Machinery. ISBN 9781450366755. doi:
495 10.1145/3308560.3317083. URL <https://doi.org/10.1145/3308560.3317083>.

496 Tianyi Bai, Hao Liang, Binwang Wan, Ling Yang, Bozhou Li, Yifan Wang, Bin Cui, Conghui He,
497 Binhang Yuan, and Wentao Zhang. A survey of multimodal large language model from a data-
498 centric perspective. *CorR*, 2024.

499 Su Lin Blodgett, Solon Barocas, Hal Daumé III, and Hanna Wallach. Language (technology) is
500 power: A critical survey of “bias” in NLP. In Dan Jurafsky, Joyce Chai, Natalie Schluter, and
501 Joel Tetreault (eds.), *Proceedings of the 58th Annual Meeting of the Association for Compu-
502 tational Linguistics*, pp. 5454–5476, Online, July 2020. Association for Computational Linguis-
503 tics. doi: 10.18653/v1/2020.acl-main.485. URL <https://aclanthology.org/2020.acl-main.485>.

504 Akash Bonagiri, Lucen Li, Rajvardhan Oak, Zeerak Babar, Magdalena Wojcieszak, and Anshu-
505 man Chhabra. Towards safer social media platforms: Scalable and performant few-shot harmful
506 content moderation using large language models. *arXiv preprint arXiv:2501.13976*, 2025.

507 Sergio G. Burdisso, Marcelo Errecalde, and Manuel Montes-y Gómez. A text classification frame-
508 work for simple and effective early depression detection over social media streams. *Expert
509 Systems with Applications*, pp. 182–197, Nov 2019. doi: 10.1016/j.eswa.2019.05.023. URL
<http://dx.doi.org/10.1016/j.eswa.2019.05.023>.

510 Weilin Cai, Juyong Jiang, Fan Wang, Jing Tang, Sunghun Kim, and Jiayi Huang. A survey on
511 mixture of experts. *Authorea Preprints*, 2024.

512 Weipeng Cao, Yuhao Wu, Yixuan Sun, Haigang Zhang, Jin Ren, Dujuan Gu, and Xingkai Wang.
513 A review on multimodal zero-shot learning. *Wiley Interdisciplinary Reviews: Data Mining and
514 Knowledge Discovery*, 13(2):e1488, 2023.

515 Tommaso Caselli, Valerio Basile, Jelena Mitrović, and Michael Granitzer. Hatebert: Retraining bert
516 for abusive language detection in english. *arXiv preprint arXiv:2010.12472*, 2020.

517 Shaoxiang Chen, Zequn Jie, and Lin Ma. Llava-mole: Sparse mixture of lora experts for mitigating
518 data conflicts in instruction finetuning mllms. *arXiv preprint arXiv:2401.16160*, 2024.

519 Jacob Devlin, Ming-Wei Chang, Kenton Lee, and Kristina Toutanova. Bert: Pre-training of deep
520 bidirectional transformers for language understanding. In *Proceedings of the 2019 conference of
521 the North American chapter of the association for computational linguistics: human language
522 technologies, volume 1 (long and short papers)*, pp. 4171–4186, 2019.

523 Christian Ezeibe. Hate speech and election violence in nigeria. *Journal of Asian and African
524 Studies*, 56(4):919–935, 2021. doi: 10.1177/0021909620951208. URL <https://doi.org/10.1177/0021909620951208>.

525 Tanmay Garg, Sarah Masud, Tharun Suresh, and Tanmoy Chakraborty. Handling bias in toxic
526 speech detection: A survey. *ACM Comput. Surv.*, 55(13s), July 2023. ISSN 0360-0300. doi:
527 10.1145/3580494. URL <https://doi.org/10.1145/3580494>.

528 Ismael Garrido-Muñoz , Arturo Montejo-Ráez , Fernando Martínez-Santiago , and L. Alfonso
529 Ureña-López . A survey on bias in deep nlp. *Applied Sciences*, 11(7), 2021. ISSN 2076-3417.
530 doi: 10.3390/app11073184. URL <https://www.mdpi.com/2076-3417/11/7/3184>.

540 Xavier Glorot and Yoshua Bengio. Understanding the difficulty of training deep feedforward neural
 541 networks. In *Proceedings of the thirteenth international conference on artificial intelligence and*
 542 *statistics*, pp. 249–256. JMLR Workshop and Conference Proceedings, 2010.

543

544 Isuru Gunasekara and Isar Nejadgholi. A review of standard text classification practices for multi-
 545 label toxicity identification of online content. In Darja Fišer, Ruihong Huang, Vinodkumar
 546 Prabhakaran, Rob Voigt, Zeerak Waseem, and Jacqueline Wernimont (eds.), *Proceedings of*
 547 *the 2nd Workshop on Abusive Language Online (ALW2)*, pp. 21–25, Brussels, Belgium, Oc-
 548 tober 2018. Association for Computational Linguistics. doi: 10.18653/v1/W18-5103. URL
 549 <https://aclanthology.org/W18-5103>.

550 Thomas Hartvigsen, Saadia Gabriel, Hamid Palangi, Maarten Sap, Dipankar Ray, and Ece Kamar.
 551 Toxigen: A large-scale machine-generated dataset for implicit and adversarial hate speech detec-
 552 tion. In *Proceedings of the 60th Annual Meeting of the Association for Computational Linguistics*,
 553 2022.

554 Kaiming He, Xiangyu Zhang, Shaoqing Ren, and Jian Sun. Delving deep into rectifiers: Surpassing
 555 human-level performance on imagenet classification. In *Proceedings of the IEEE international*
 556 *conference on computer vision*, pp. 1026–1034, 2015.

557 Lukas Helff, Felix Friedrich, Manuel Brack, Patrick Schramowski, and Kristian Kersting. Llava-
 558 guard: Vlm-based safeguard for vision dataset curation and safety assessment. In *Proceedings of*
 559 *the IEEE/CVF Conference on Computer Vision and Pattern Recognition*, pp. 8322–8326, 2024.

560

561 Chengsong Huang, Qian Liu, Bill Yuchen Lin, Tianyu Pang, Chao Du, and Min Lin. Lorahub: Effi-
 562 cient cross-task generalization via dynamic lora composition. *arXiv preprint arXiv:2307.13269*,
 563 2023.

564 Aaron Hurst, Adam Lerer, Adam P Goucher, Adam Perelman, Aditya Ramesh, Aidan Clark, AJ Os-
 565 trow, Akila Welihinda, Alan Hayes, Alec Radford, et al. Gpt-4o system card. *arXiv preprint*
 566 *arXiv:2410.21276*, 2024.

567

568 HuEdward J., Yulong Shen, Phillip Wallis, Zeyuan Allen-Zhu, Yuanzhi Li, Shean Wang, and Weizhu
 569 Chen. Lora: Low-rank adaptation of large language models. *arXiv: Computation and Lan-*
 570 *guage,arXiv: Computation and Language*, Jun 2021.

571 Ahmet Kaya, Oguzhan Ozcelik, and Cagri Toraman. Arc-nlp at climateactivism 2024: Stance and
 572 hate speech detection by generative and encoder models optimized with tweet-specific elements.
 573 In *Proceedings of the 7th Workshop on Challenges and Applications of Automated Extraction of*
 574 *Socio-political Events from Text (CASE 2024)*, pp. 111–117, 2024.

575

576 Robin Kowalski. Cyberbullying. In *The Routledge international handbook of human aggression*,
 577 pp. 131–142. Routledge, 2018.

578

579 Dengchun Li, Yingzi Ma, Naizheng Wang, Zhiyuan Cheng, Lei Duan, Jie Zuo, Cal Yang, and
 580 Mingjie Tang. Mixlora: Enhancing large language models fine-tuning with lora based mixture of
 581 experts. *arXiv preprint arXiv:2404.15159*, 2024.

582

583 Yinhan Liu, Myle Ott, Naman Goyal, Jingfei Du, Mandar Joshi, Danqi Chen, Omer Levy, Mike
 584 Lewis, Luke Zettlemoyer, and Veselin Stoyanov. Roberta: A robustly optimized bert pretraining
 585 approach. *arXiv preprint arXiv:1907.11692*, 2019.

586

587 Albert Lu and Stephen Cranefield. Ultra low-cost two-stage multimodal system for non-normative
 588 behavior detection. *arXiv preprint arXiv:2403.16151*, 2024.

589

590 Batta Mahesh. Machine learning algorithms-a review. *International Journal of Science and Re-*
 591 *search (IJSR). [Internet]*, 9(1):381–386, 2020.

592

593 Saeed Masoudnia and Reza Ebrahimpour. Mixture of experts: a literature survey. *Artificial Intelli-*
 594 *gence Review*, 42:275–293, 2014.

Ahmed Cherif Mazari, Nesrine Boudoukhani, and Abdelhamid Djeffal. Bert-based ensemble learn-
 595 ing for multi-aspect hate speech detection. *Cluster Computing*, 27(1):325–339, 2024.

594 Yiting Qu, Xinyue Shen, Yixin Wu, Michael Backes, Savvas Zannettou, and Yang Zhang. Un-
 595 safebench: Benchmarking image safety classifiers on real-world and ai-generated images. *arXiv*
 596 *preprint arXiv:2405.03486*, 2024.

597 Alec Radford, Jong Wook Kim, Chris Hallacy, Aditya Ramesh, Gabriel Goh, Sandhini Agarwal,
 598 Girish Sastry, Amanda Askell, Pamela Mishkin, Jack Clark, et al. Learning transferable visual
 599 models from natural language supervision. In *International conference on machine learning*, pp.
 600 8748–8763. PMLR, 2021.

601 Robin Rombach, Andreas Blattmann, Dominik Lorenz, Patrick Esser, and Björn Ommer. High-
 602 resolution image synthesis with latent diffusion models, 2021.

603 Mohammad Salama, Jonathan Kahana, Eliahu Horwitz, and Yedid Hoshen. Dataset size recovery
 604 from lora weights. *arXiv preprint arXiv:2406.19395*, 2024.

605 Victor Sanh, Lysandre Debut, Julien Chaumond, and Thomas Wolf. Distilbert, a distilled version of
 606 bert: smaller, faster, cheaper and lighter. *arXiv preprint arXiv:1910.01108*, 2019.

607 Maarten Sap, Saadia Gabriel, Lianhui Qin, Dan Jurafsky, Noah A Smith, and Yejin Choi. So-
 608 cial bias frames: Reasoning about social and power implications of language. *arXiv preprint*
 609 *arXiv:1911.03891*, 2019.

610 Shuvam Shiwakoti, Surendrabikram Thapa, Kritesh Rauniyar, Akshyat Shah, Aashish Bhandari, and
 611 Usman Naseem. Analyzing the dynamics of climate change discourse on twitter: A new annotated
 612 corpus and multi-aspect classification. In *Joint 30th International Conference on Computational*
 613 *Linguistics and 14th International Conference on Language Resources and Evaluation, LREC-*
 614 *COLING 2024*, pp. 984–994. European Language Resources Association (ELRA), 2024.

615 Reza Shokri, Marco Stronati, Congzheng Song, and Vitaly Shmatikov. Membership inference at-
 616 tacks against machine learning models. In *2017 IEEE symposium on security and privacy (SP)*,
 617 pp. 3–18. IEEE, 2017.

618 CK Singh, N Pavithra, and Renu Joshi. Internet an integral part of human life in 21st century: a
 619 review. *Current Journal of Applied Science and Technology*, 41(36):12–18, 2022a.

620 Inderpreet Singh, Gulshan Goyal, and Anmol Chandel. Alexnet architecture based convolu-
 621 tional neural network for toxic comments classification. *Journal of King Saud University*
 622 - *Computer and Information Sciences*, 34(9):7547–7558, 2022b. ISSN 1319-1578. doi:
 623 <https://doi.org/10.1016/j.jksuci.2022.06.007>. URL <https://www.sciencedirect.com/science/article/pii/S1319157822002026>.

624 Ravinder Singh, Sudha Subramani, Jiahua Du, Yanchun Zhang, Hua Wang, Yuan Miao, and Khan-
 625 dakter Ahmed. Antisocial behavior identification from twitter feeds using traditional machine
 626 learning algorithms and deep learning. *EAI Endorsed Transactions on Scalable Information Sys-*
 627 *tems*, 10(4), 5 2023. doi: 10.4108/eetsis.v10i3.3184.

628 Libo Sun, Siyuan Wang, Xuanjing Huang, and Zhongyu Wei. Identity-driven hierarchical role-
 629 playing agents. *arXiv preprint arXiv:2407.19412*, 2024.

630 Yi-Lin Sung, Jaemin Cho, and Mohit Bansal. Vi-adapter: Parameter-efficient transfer learning
 631 for vision-and-language tasks. In *2022 IEEE/CVF Conference on Computer Vision and Pattern*
 632 *Recognition (CVPR)*, Jun 2022. doi: 10.1109/cvpr52688.2022.00516. URL <http://dx.doi.org/10.1109/cvpr52688.2022.00516>.

633 Gemma Team, Thomas Mesnard, Cassidy Hardin, Robert Dadashi, Surya Bhupatiraju, Shreya
 634 Pathak, Laurent Sifre, Morgane Rivière, Mihir Sanjay Kale, Juliette Love, et al. Gemma: Open
 635 models based on gemini research and technology. *arXiv preprint arXiv:2403.08295*, 2024.

636 Betty Van Aken, Julian Risch, Ralf Krestel, and Alexander Löser. Challenges for toxic comment
 637 classification: An in-depth error analysis. *arXiv preprint arXiv:1809.07572*, 2018.

638 Bertie Vidgen, Tristan Thrush, Zeerak Waseem, and Douwe Kiela. Learning from the worst: Dy-
 639 namically generated datasets to improve online hate detection. *arXiv preprint arXiv:2012.15761*,
 640 2020.

648 Nicolas Webersinke, Matthias Kraus, Julia Anna Bingler, and Markus Leippold. Climatebert: A
 649 pretrained language model for climate-related text. *arXiv preprint arXiv:2110.12010*, 2021.
 650

651 Laura Weidinger, John Mellor, Maribeth Rauh, Conor Griffin, Jonathan Uesato, Po-Sen Huang,
 652 Myra Cheng, Mia Glaese, Borja Balle, Atoosa Kasirzadeh, et al. Ethical and social risks of harm
 653 from language models. *arXiv preprint arXiv:2112.04359*, 2021.

654 Xun Wu, Shaohan Huang, and Furu Wei. Mixture of lora experts. *arXiv preprint arXiv:2404.13628*,
 655 2024.

656

657 An Yang, Baosong Yang, Binyuan Hui, Bo Zheng, Bowen Yu, Chang Zhou, Chengpeng Li,
 658 Chengyuan Li, Dayiheng Liu, Fei Huang, Guanting Dong, Haoran Wei, Huan Lin, Jialong Tang,
 659 Jialin Wang, Jian Yang, Jianhong Tu, Jianwei Zhang, Jianxin Ma, Jin Xu, Jingren Zhou, Jinze Bai,
 660 Jinzheng He, Junyang Lin, Kai Dang, Keming Lu, Keqin Chen, Kexin Yang, Mei Li, Mingfeng
 661 Xue, Na Ni, Pei Zhang, Peng Wang, Ru Peng, Rui Men, Ruize Gao, Runji Lin, Shijie Wang, Shuai
 662 Bai, Sinan Tan, Tianhang Zhu, Tianhao Li, Tianyu Liu, Wenbin Ge, Xiaodong Deng, Xiaohuan
 663 Zhou, Xingzhang Ren, Xinyu Zhang, Xipin Wei, Xuancheng Ren, Yang Fan, Yang Yao, Yichang
 664 Zhang, Yu Wan, Yunfei Chu, Yuqiong Liu, Zeyu Cui, Zhenru Zhang, and Zhihao Fan. Qwen2
 665 technical report. *arXiv preprint arXiv:2407.10671*, 2024.

666

667 Chen Yeh, You-Ming Chang, Wei-Chen Chiu, and Ning Yu. T2vs meet vlms: A scalable multimodal
 668 dataset for visual harmfulness recognition. *Advances in Neural Information Processing Systems*,
 37:112950–112961, 2024.

669

670 Jaehong Yoon, Shoubin Yu, Vaidehi Patil, Huaxiu Yao, and Mohit Bansal. Safree: Training-free
 671 and adaptive guard for safe text-to-image and video generation, 2025. URL <https://arxiv.org/abs/2410.12761>.

672

673 Greysen K Young. How much is too much: the difficulties of social media content moderation.
 674 *Information & Communications Technology Law*, 31(1):1–16, 2022.

675

676 MD Zeiler. Visualizing and understanding convolutional networks. In *European conference on
 677 computer vision/arXiv*, volume 1311, 2014.

678

679 Wenjun Zeng, Dana Kurniawan, Ryan Mullins, Yuchi Liu, Tamoghna Saha, Dirichi Ike-Njoku,
 680 Jindong Gu, Yiwen Song, Cai Xu, Jingjing Zhou, et al. Shieldgemma 2: Robust and tractable
 681 image content moderation. *arXiv preprint arXiv:2504.01081*, 2025.

682

683 Ming Zhong, Yelong Shen, Shuohang Wang, Yadong Lu, Yizhu Jiao, Siru Ouyang, Donghan Yu,
 684 Jiawei Han, and Weizhu Chen. Multi-lora composition for image generation. *arXiv preprint
 685 arXiv:2402.16843*, 2024.

686

687 Yanqi Zhou, Tao Lei, Hanxiao Liu, Nan Du, Yanping Huang, Vincent Zhao, Andrew M Dai, Quoc V
 688 Le, James Laudon, et al. Mixture-of-experts with expert choice routing. *Advances in Neural
 689 Information Processing Systems*, 35:7103–7114, 2022.

690

691 Elizaveta Zinov'yeva, Wolfgang Karl Härdle, and Stefan Lessmann. Antisocial online behavior de-
 692 tected using deep learning. *Decision Support Systems*, 138:113362, 2020. ISSN 0167-9236.
 693 doi: <https://doi.org/10.1016/j.dss.2020.113362>. URL <https://www.sciencedirect.com/science/article/pii/S0167923620301172>.

694

695

696

697

698

699

700

701

702 **A RELATED WORK**

703

704 We situate MoLD within existing research by briefly reviewing challenges in multimodal detection,
 705 the evolution of automated detection methods, approaches to multi-risk handling, and the novel
 706 application of weight-based analysis, thereby highlighting MoLD’s contributions.

707 **Data Scalability in Multimodal Risk Detection.** A significant challenge in effectively detecting
 708 risks across diverse modalities like text and images Lu & Cranefield (2024); Yoon et al. (2025) is
 709 the extensive data typically required for training robust models, often involving complex annotation
 710 efforts Bai et al. (2024); Van Aken et al. (2018). MoLD directly addresses this data scalability issue
 711 through its emphasis on a highly data-efficient learning paradigm.

712 **Automated Toxicity Detection.** While advanced architectures such as Pre-trained Language
 713 Models (PLMs) like BERT Mazari et al. (2024) and vision models like CLIP Radford et al. (2021)
 714 significantly improved contextual understanding and detection accuracy, their effectiveness often
 715 relies on large labeled datasets Mahesh (2020). This reliance has spurred the development of more
 716 data-efficient techniques, including few-shot Bonagiri et al. (2025); Yeh et al. (2024) and zero-shot
 717 learning Cao et al. (2023); AlDahoul et al. (2024). MoLD strategically adopts such data-efficient
 718 principles to enhance its practical applicability in resource-constrained scenarios.

719 **Approaches for Multi-Risk Detection.** Mixture of Experts (MoE) models Masoudnia &
 720 Ebrahimpour (2014); Cai et al. (2024), including LoRA-based variants Chen et al. (2024); Li et al.
 721 (2024); Wu et al. (2024), often manage multiple risks by routing or mitigating expert interference
 722 Zhou et al. (2022), typically avoiding direct expert conflicts Zhong et al. (2024); Sun et al.
 723 (2024). MoLD distinctively analyzes the dynamic weight interplay among multiple thematic groups
 724 of LoRA modules, which are intentionally extreme-trained on different tendencies. This assessment
 725 through a compositional analysis of these tendencies, rather than expert selection or simple
 726 composition Sung et al. (2022); Huang et al. (2023).

727 **Risk Assessment via Weight Analysis.** Learned model weights Glorot & Bengio (2010); He
 728 et al. (2015) can encode valuable information beyond their primary predictive function Zeiler (2014).
 729 While some research explores LoRA weight analysis for auxiliary tasks (e.g., inferring dataset prop-
 730 erties Salama et al. (2024); Shokri et al. (2017)), MoLD innovatively applies this concept for direct
 731 risk assessment. It analyzes dynamically optimized scalar weights—which modulate the influence
 732 of extreme-trained LoRA modules J. et al. (2021), to classify, localize, and score toxicity, forming
 733 the core of its interpretable, fine-grained evaluation capabilities.

734
 735
 736
 737
 738
 739
 740
 741
 742
 743
 744
 745
 746
 747
 748
 749
 750
 751
 752
 753
 754
 755